NASA/TM—2013-217889

Advances in SiC/SiC Composites for Aero-Propulsion

James A. DiCarlo
Glenn Research Center, Cleveland, Ohio

July 2013

NASA STI Program . . . in Profile

Since its founding, NASA has been dedicated to the advancement of aeronautics and space science. The NASA Scientific and Technical Information (STI) program plays a key part in helping NASA maintain this important role.

The NASA STI Program operates under the auspices of the Agency Chief Information Officer. It collects, organizes, provides for archiving, and disseminates NASA's STI. The NASA STI program provides access to the NASA Aeronautics and Space Database and its public interface, the NASA Technical Reports Server, thus providing one of the largest collections of aeronautical and space science STI in the world. Results are published in both non-NASA channels and by NASA in the NASA STI Report Series, which includes the following report types:

- TECHNICAL PUBLICATION. Reports of completed research or a major significant phase of research that present the results of NASA programs and include extensive data or theoretical analysis. Includes compilations of significant scientific and technical data and information deemed to be of continuing reference value. NASA counterpart of peer-reviewed formal professional papers but has less stringent limitations on manuscript length and extent of graphic presentations.

- TECHNICAL MEMORANDUM. Scientific and technical findings that are preliminary or of specialized interest, e.g., quick release reports, working papers, and bibliographies that contain minimal annotation. Does not contain extensive analysis.

- CONTRACTOR REPORT. Scientific and technical findings by NASA-sponsored contractors and grantees.

- CONFERENCE PUBLICATION. Collected papers from scientific and technical conferences, symposia, seminars, or other meetings sponsored or cosponsored by NASA.

- SPECIAL PUBLICATION. Scientific, technical, or historical information from NASA programs, projects, and missions, often concerned with subjects having substantial public interest.

- TECHNICAL TRANSLATION. English-language translations of foreign scientific and technical material pertinent to NASA's mission.

Specialized services also include creating custom thesauri, building customized databases, organizing and publishing research results.

For more information about the NASA STI program, see the following:

- Access the NASA STI program home page at *http://www.sti.nasa.gov*

- E-mail your question to *help@sti.nasa.gov*

- Fax your question to the NASA STI Information Desk at 443–757–5803

- Phone the NASA STI Information Desk at 443–757–5802

- Write to:
  STI Information Desk
  NASA Center for AeroSpace Information
  7115 Standard Drive
  Hanover, MD 21076–1320

NASA/TM—2013-217889

Advances in SiC/SiC Composites for Aero-Propulsion

James A. DiCarlo
Glenn Research Center, Cleveland, Ohio

National Aeronautics and
Space Administration

Glenn Research Center
Cleveland, Ohio 44135

July 2013

Acknowledgments

Regarding the SiC/SiC advancements made over the last decade, the author gratefully acknowledges the funding support of the NASA Ultra Efficient Engine Technology program, the NASA Glenn Director's Discretionary Fund, and the NASA Fundamental Aeronautics program. As major contributors to these advancements, the author wishes to acknowledge the exceptional professional efforts of H.M. Yun, R.T. Bhatt, and G.N. Morscher, plus the excellent technical support of R. Phillips, R. Babuder, and R. Angus.

Level of Review: This material has been technically reviewed by technical management.

Available from

NASA Center for Aerospace Information
7115 Standard Drive
Hanover, MD 21076–1320

National Technical Information Service
5301 Shawnee Road
Alexandria, VA 22312

Available electronically at http://www.sti.nasa.gov

Advances in SiC/SiC Composites for Aero-Propulsion

James A. DiCarlo
National Aeronautics and Space Administration
Glenn Research Center
Cleveland, Ohio 44135

Abstract

In the last decade, considerable progress has been made in the development and application of ceramic matrix composites consisting of silicon carbide (SiC) based matrices reinforced by small-diameter continuous-length SiC-based fibers. For example, these SiC/SiC composites are now in the early stages of implementation into hot-section components of civil aero-propulsion gas turbine engines, where in comparison to current metallic components they offer multiple advantages due to their lighter weight and higher temperature structural capability. For current production-ready SiC/SiC, this temperature capability for long time structural applications is ~1250 °C, which is better than ~1100 °C for the best metallic superalloys. Foreseeing that even higher structural reliability and temperature capability would continue to increase the advantages of SiC/SiC composites, progress in recent years has also been made at NASA toward improving the properties of SiC/SiC composites by optimizing the various constituent materials and geometries within composite microstructures. The primary objective of this chapter is to detail this latter progress, both fundamentally and practically, with particular emphasis on recent advancements in the materials and processes for the fiber, fiber coating, fiber architecture, and matrix, and in the design methods for incorporating these constituents into SiC/SiC microstructures with improved thermo-structural performance.

1.0 Introduction

Silicon carbide (SiC) ceramic matrix composites (CMC) reinforced by continuous-length, high-performance, small-diameter (~10 to 15 μm), polycrystalline SiC fibers are considered enabling materials for a variety of advanced applications where lightweight re-usable structural materials are required to operate for long time periods within extreme high-temperature environments. Today the first generations of SiC/SiC CMC with thermo-structural capability to ~1250 °C are being introduced into the hot-section components of military and commercial gas turbine engines (Refs. 1 and 2). In comparison to superalloy metallic components, which at best operate as high as ~1100 °C, these CMC components will not only offer reduced engine weight, but also reduced component cooling-air requirements. Reduction in cooling air would then have the additional engine benefits of improved thrust-to-weight ratio, reduced fuel burn, and reduced harmful exhaust emissions. In order to seek further increases in these engine benefits, research has been on-going within NASA aimed at developing SiC/SiC CMC with even higher structural reliability and temperature capability.

The objective of this chapter is to detail, both fundamentally and practically, the key advances from recent SiC/SiC CMC research activities within NASA. Although these advances are primarily still under development and optimization, they do show various degrees of improvement over the materials and processes currently being implemented for SiC/SiC engine components. To this end, Section 2.0 of this chapter presents information on the general constituent materials and process requirements for structurally reliable high-temperature SiC/SiC engine components. Section 3.0 then discusses the primary fabrication routes currently being employed for production-ready SiC/SiC components in terms of their benefits and limitations. Section 4.0 then details recent advancements in the materials and processes for the SiC fiber, the fiber interfacial coating, the fiber geometry or architecture, the SiC-based matrix, and in the design methods for assembling these microstructural constituents into higher-temperature higher-performance SiC/SiC composites and components. Where possible, CMC property data will be presented and analyzed

that directly compares the materials and processes of the advanced approaches against those of current approaches. This property comparison will focus primarily on such key CMC properties as in-plane and thru-thickness tensile strength, thermal conductivity, creep resistance, and rupture behavior since it is these properties that directly control the CMC structural and upper temperature capability. Finally Section 5.0 summarizes these results into current design guidelines for achieving SiC/SiC microstructures with improved intrinsic thermo-structural capability, and then discusses potential issues, such as thermo-mechanical shock, environmental attack, and creep-related residual stress development, which still require further research to understand whether they will be areas of concern for real engine components.

2.0 Materials and Process Requirements for Structurally Reliable High-Temperature SiC/SiC Components

As with any structural ceramic material, the first key performance requirement for a SiC/SiC CMC is the ability to display three-dimensional (3D) strength properties or allowables that are high enough to permit a component to achieve its desired service life. Like metallic hot-section components, ceramic components for aero-propulsion gas turbine engines will typically be designed to be thin-walled and cooled using conventional approaches such as film cooling (vanes, blades) and backside convective cooling (combustion liners, shrouds). Thus component stresses typically arise from a combination of mechanical, aerodynamic, and thermal-gradient loads that produce both in-plane and thru-thickness stress-temperature distributions that can vary with time within the component walls and attachment areas. Under these stress conditions over a time period generally equivalent to the component inspection cycle, the SiC/SiC composite's in-plane Matrix Cracking Strength (MCS) should be sufficiently high enough to reliably avoid cracks that propagate into and across the component wall, thereby preventing aggressive application environments from reaching and degrading the crack-bridging fibers. Of additional importance is the ability of the CMC to avoid the occurrence of delamination cracks within the wall since these can significantly reduce the thru-thickness thermal conductivity, further increasing the thermal gradient stresses and the probability of wall spallation. Thus the constituents and geometries of the as-produced CMC should be optimized to assure that the composite's matrix cracking strengths both in-plane and thru-thickness sufficiently exceed the expected component service stresses in these directions.

In terms of maintaining these 3D strength characteristics *at high temperatures*, the key requirements of the SiC/SiC fiber and matrix constituents are (1) to be thermally stable at the expected application temperatures and (2) to avoid fracture under the maximum time, temperature, and stress conditions that they will experience during component service. Today these constituents will most always have a polycrystalline SiC microstructure in part due to the fact that single crystal microstructures are too costly to produce. Also, as seen for single crystal oxide fibers in oxide matrices, single crystal microstructures may not offer any significant performance advantage over polycrystalline materials due to rapid atomic diffusion on the fiber surface and pitting-induced fiber strength loss caused by irregular contact points with the multiconstituents in the composite environment (Ref. 3). Furthermore, if the SiC fiber and matrix contain a pure stoichiometric composition and grain sizes near ~500 nm, their intrinsic microstructural and strength stability under zero stress conditions is not an issue for thousands of hours at temperatures up to at least 1600 °C. However, as soon as stress is applied to a SiC/SiC component, the grains in the constituent microstructures will begin to slide past each other, giving rise to measurable time-dependent deformation or creep that could start as low as ~1100 °C depending on the impurity phases in the grain boundaries. Two practical issues with constituent creep are undesirable dimensional changes for the CMC component and the growth of cavitation flaws at the grain triple points within the constituent microstructures. Eventually these flaws grow large enough to cause time-dependent constituent fracture or rupture, which in the worst case could cause rupture of the total SiC/SiC component. Unlike metals that can rupture at creep strains well over 1 percent so that undesirable dimensional changes are typically their life limiting criteria, SiC-based constituents will typically rupture at strains below 1 percent so that their use lives are primarily limited by rupture rather than by dimensional stability issues. Thus for

structurally reliable high-temperature operation for long times, the constituents of SiC/SiC composites should have microstructures and compositions that display the optimum in creep and rupture resistance under the stress and temperature conditions that they will encounter within the final application.

Another life-limiting and creep-related mechanism for high-temperature SiC/SiC components is that the constituents almost always differ in creep behavior due to different compositions and/or to different stresses related to their geometries within the composite. To appreciate this issue, one can consider the situation where a constant and uniform mechanical load is applied to a composite and the fiber and matrix within the composite display significantly different creep behavior. For Case A, where the matrix is more creep prone than fiber, the matrix will relax its initial stress and shed more of the CMC load onto the fibers, so that the composite upper use temperature will then typically depend on such life-limiting issues as excessive fiber deformation, fiber time-dependent fracture or rupture, and/or adverse residual stress development within the composite. Regarding this last issue, after creep under uniform CMC tensile loads, the internal residual stress on the matrix at lower temperatures will be compressive, so that the CMC in-plane MCS will beneficially increase in this temperature regime (Ref. 4). However, after CMC creep under compressive loads, tensile residual stresses on the matrix will develop at lower temperatures, thereby decreasing the CMC MCS at these lower temperatures and increasing the chance of thru-thickness cracking if the local CMC load should become tensile. This reduction in MCS has been shown to be a likely scenario for components with non-uniform stresses in their walls, as for example when subject to thermal gradients across the walls (Ref. 5). As will be discussed, this Case A scenario is the situation with current SiC/SiC composites containing free silicon in the matrix. For Case B, where the matrix is more creep resistant than the fiber, the fiber in its primary creep stage will quickly shed its load to the matrix, so that initial composite tensile loads must be kept low to avoid the matrix stresses rising over time above their cracking limit. Bottom line is that, if possible, both the fiber and matrix should be highly creep resistant under the component service conditions; but if this is not the case, the matrix creep should be slightly greater than that of the fiber, so that during the component service life, the matrix carries some of the composite load and remains protective of the fiber without cracking.

3.0 Current Fabrication Routes for SiC/SiC Engine Components

Today two primary SiC/SiC fabrication routes have achieved to a large degree the material and process requirements needed to produce complex-shaped engine components with microstructures capable of reliable structural operation for long times at temperatures greater than those of metallic superalloys. The first route was developed under the NASA Enabling Propulsion Materials (EPM) Program and was demonstrated by the production of small and large combustor liners (Ref. 6). Here continuous-length multifiber tows of a small-diameter high-performance SiC fiber type are woven into continuous fabric pieces, typically with a 0/90 balanced five-harness satin (5HS) fiber architecture. These two-dimensional (2D) fabric pieces are then cut and judiciously stacked into component-shaped 3D pre-forms with fiber volume fractions up to 40 percent. Chemical vapor infiltration (CVI) is employed to first apply an interfacial coating or interphase on the fibers within the tows, and then to apply a thin protective SiC matrix layer over the interphase. To adequately achieve the key interfacial coating requirements of high environmental durability and high compliance for matrix crack deflection, the interphase composition is typically based on silicon-doped boron nitride (BN). The coating thicknesses can vary from ~0.1 to 0.5 μm depending on such factors as the fiber surface roughness and the degree of protection needed to avoid coating degradation during matrix formation and/or component service. The thin CVI SiC matrix coating is important in that it not only protects the interphase and fibers from subsequent matrix infiltration processes and from external environments, but it also provides a highly thermally conductive and creep-resistant matrix constituent. As will be discussed, NASA has determined that these latter two matrix properties, as well as the protective nature of the interface coating, can be further improved prior to the final matrix infiltration steps by a high temperature treatment of the CVI SiC-coated pre-form (Ref. 7). In the final steps of matrix fabrication, SiC particulate is slurry-cast into the component pre-form near room temperature, followed by a finishing step in which a molten metallic silicon alloy is

infiltrated near 1400 °C into any open remaining matrix porosity. The silicon bonds the SiC particulates together with little chemical reaction. This last step of this non-reactive melt infiltration (NRMI) route is important in that it results in a SiC-based matrix with low residual porosity, high thermal conductivity, and good environmental protection for the coated fibers. In addition, it minimizes the existence of large matrix flaws, thereby raising the stress levels required for formation of detrimental thru-thickness and delamination cracks in the composite. In following discussions, the matrices formed from the NRMI approach of CVI, slurry, and silicon melt infiltration (MI) will often be referred to as the CVI-MI matrices for simplicity.

In the second fabrication route, which has been developed and demonstrated by General Electric for a variety of turbine hot-section components, multifiber tows of a small-diameter high-performance SiC fiber type are first spread and coated by chemical vapor deposition (CVD) with a layered interfacial coating consisting of BN and silicon nitride (Si_3N_4) compositions (Ref. 8). The coated tows are then pre-pregged into unidirectional 2D tapes using a polymer-based binder containing SiC and carbon particulates. The tapes are then cut, oriented, and stacked into 3D pre-forms with total fiber volume content less than 30 percent. To achieve the component structural and shape requirements, the 3D pre-forms are assembled using methods much like those used for tape lay-up of polymer matrix composites. In the final steps of this "prepreg" approach, the 3D pre-form is heated to high temperature to decompose the polymer and to form the final matrix composition by infiltration with molten silicon near. Unlike the NMI route, the SiC-based matrix is formed in-situ by the reaction of the silicon with the residual carbon in the preform. During this reactive MI (RMI) process, there is an exothermic reaction between silicon and carbon, resulting in an expansion of the matrix that puts the fibers under residual tension and the final matrix under residual compression, which is beneficial in increasing the composite in-plane cracking strength at low temperatures. However, the RMI route also causes a rise in local temperatures, which if not controlled could cause strength loss in those SiC fiber types that are produced at maximum temperatures near 1400 °C. In addition, unless the interphase coating is thick enough (~1 μm) with the proper compositions, these temperature increases can increase the risk of fiber attack by the thermally-induced diffusion of excess free silicon across the coating. Thus SiC fibers with the highest production temperatures are generally preferred for strength retention during both the NRMI and RMI matrix fabrication routes.

In terms of temperature capability, both current CMC fabrication routes always result in some excess silicon in the matrix, thereby allowing SiC/SiC components under their application loads to display undesirable matrix creep that begins at ~1100 °C, and becomes excessive above ~1300 °C. As described in Case A above, if the SiC fiber is more creep resistant than these matrices, effectively all the composite load will be shifted to the fiber, resulting in composite creep and rupture at the higher temperatures controlled by the fiber creep-rupture characteristics and its volume fractions. In addition, at temperatures approaching ~1400 °C, not only does the excess silicon melt and tend to exude from the composite, but the beneficial residual stresses in the RMI route will tend to disappear. Thus for current production SiC/SiC composites fabricated by both MI routes and with high-temperature SiC fibers, it is the final silicon infiltration step and not the reinforcing SiC fiber that is the prime mechanism that limits the intrinsic CMC upper use temperature to only ~1250 °C.

4.0 Recent NASA Advancements in SiC/SiC Materials and Processes

Although the current CMC fabrication routes described above are adequate for the introduction of SiC/SiC components into the hot sections of aero-propulsion turbine engines, NASA has determined that these production approaches not offer the optimum in SiC/SiC composite structural reliability or in high temperature service capability. The following sections will detail the various deficiencies of these routes and the advancement approaches recently developed by NASA and demonstrated with industry collaboration to address these short-comings.

4.1 Advances in SiC-Based Fibers

First-level property requirements for a SiC fiber in high-performance high-temperature SiC/SiC components are (1) to be produced in continuous lengths with a small diameter; (2) to display in its as-produced condition high tensile strength (~3 GPa) and high-stiffness or modulus (~400 GPa); and (3) to have the ability to retain as much of this strength and stiffness as possible at high temperatures for long times under high stresses. Today the best approach for achieving these requirements is by the spinning, curing, and pyrolysis of multifilament tows of polymer derived fibers (Ref. 9). For high strength and stiffness in their as-produced condition, key fiber microstructural requirements are, respectively, average grain sizes below ~500 nm and a near- stoichiometric SiC composition with high density (>3.0 gm/cm^3) or low porosity (Ref. 10). Although decreasing grain size below 500 nm should theoretically increase tensile strength of polymer-derived SiC fibers, this is not observed because inherent in the polymer preparation and spinning processes, flaw-related particulates with sizes of the order of ~200 nm are allowed to pass into the green fibers. Thus for the finer grained SiC fibers, these particulates rather than the fiber grains are limiting the strength to ~3 GPa. For high strength and stiffness retention (creep resistance) during service at high temperatures, key microstructural requirements are a pure near-stoichiometric SiC composition and grain sizes as large as possible without exceeding ~500 nm. These properties in turn will also provide a SiC fiber with high intrinsic thermal conductivity (>50 W/m.K), a property very important for cooled components. Finally, on the more practical side, the SiC fiber should be commercially available in large quantities and with low acquisition or life-cycle cost.

Today the commercial SiC fiber type that is primarily being employed for both the NRMI and RMI SiC/SiC component fabrication approaches is the “Hi-Nicalon Type S” fiber (hereafter HNS fiber) that is produced by Nippon Carbon in Japan. This fiber meets most of the fiber practical requirements, particularly commercial availability in large quantities (Ref. 2), but still lacks some important microstructural requirements. The HNS fiber, like its “Hi-Nicalon” precursor fiber, is first spun from a organometallic “pre-ceramic” polymer precursor, followed by cross-linking or curing under electron irradiation. It is then subjected to high-temperature pyrolysis and heat treatment steps to remove the excess carbon present in the Hi-Nicalon fiber (C/Si~1.3) and to form a nearly stoichiometric (C/Si~1.05) β-phase SiC fiber (Ref. 11). Some key chemical and physical properties for the as-produced HNS fiber are shown in Table 1, and compared with other SiC-based fibers with potential for high-temperature CMC (Refs. 9, 11 to 14). Even though irradiation rather than oxidative curing is employed, the HNS fiber still contains residual oxygen (~0.7 wt%), which typically is in the form of a silicon-oxycarbide impurity phase. When exposed for short times at temperatures greater than ~1600 °C, this phase decomposes into SiO and CO gases, which in turn creates pores in the fiber, thereby reducing fiber strength (Ref. 15). In addition, the as-produced HNS (NOX grade) fiber has a carbon-rich surface, which can be detrimentally removed within the CMC when exposed to combustion environments (Ref. 16). Thus for turbine applications, a judicious practice is to utilize HNS (OX grade) fibers where the carbon surface has been removed by the fiber vendor or by the fiber end-user prior to CMC fabrication. However, as shown in Table 1, this will reduce fiber strength by ~10 percent by exposing flaws on the as-produced fiber surface. Adding a compliant interfacial coating to the fiber, such as BN, may act to blunt these flaws again, provided the coating is applied to all areas of the fiber surface.

Regarding structural performance at high temperatures, because of its thermal limit of ~1600 °C for strength retention, the average grain size within the as-produced HNS fiber does not grow beyond ~20 nm (Ref. 9) and the fiber still retains the oxide-based impurity phase in its grain boundaries (Ref. 12). Recent studies at NASA (Ref. 17) suggest that these two factors are the prime contributors to undesirable fiber creep and a structural limit for this fiber type of less than ~1450 °C. To better understand this limitation, Figure 1 compares the creep behavior of various polymer-derived SiC fiber types when subjected as single fibers to a constant stress (σ) of 270 MPa at a constant high-temperature (**T**) of 1400 °C in laboratory air (Ref. 17). One can see that all polycrystalline SiC fibers display a time-dependent transient or primary creep strain (ε_p) followed by a nearly steady-state secondary creep strain (ε_s). NASA (Refs. 10

and 17) has identified the underlying creep mechanism for the secondary stage of these fine grained SiC fibers as Interface Controlled Diffusional (ICD) creep in which the concentration of vacancies supporting fiber creep by grain-boundary diffusion is limited by the fine-sized grains (Ref. 18). In this case, the second stage creep strain rate ($\dot{\varepsilon}_s$) can be described analytically as:

$$\varepsilon_s = (C/d)\sigma^3 \exp[-Q/RT] \quad (1)$$

TABLE 1.—SOME KEY PROPERTIES OF SiC-BASED FIBERS FOR HIGH TEMPERATURE SiC/SiC CMC

Fiber type (Trade-Name)	Vendor	Max temp.[a]	Key Non-SiC elements in bulk, wt.%	Grain size [b], nm	Key surface phase	Tensile strength [c], GPa	R.T. thermal cond., W/m.K	Ref.
Hi-Nicalon	Nippon Carbon	1450 °C	0.5 Ox	[d]5	C	3.0	8	9, 11
Hi-Nicalon Type-S (NOX grade)	Nippon Carbon	1650 °C	0.7 Ox	[d]20	C	2.8	18	9, 12
Hi-Nicalon Type-S (OX grade)	Nippon Carbon	1650 °C	0.7 Ox	[d]20	SiC	2.6	18	12
Sylramic	ATK-COI Ceramics	1850 °C	< 0.1 Ox, 1.2 B, 2.4 Ti	100	B	3.2	46	13
Sylramic-iBN	ATK-COI Ceramics	1800 °C	< 0.1 Ox, ~0 B, 2.4 Ti	200	BN	3.1	> 50	13
Super Sylramic-iBN	NASA	1800 °C	< 0.1 Ox, ~0 B, 2.4 Ti	200	BN	3.0	> 50	14
Tyranno SA3	UBE Industries	1900 °C	0.2 Ox, 0.6 Al	400	SiC	2.8	65	9

[a]~Maximum temperature for loss of >10 percent of as-produced strength after 10 hr inert exposure
[b]~Average grain size measured by TEM
[c]Average as-produced single fiber strength at room temperature and 25 mm gauge length
[d]Spinning-related strength controlling flaws are ~200 nm in size

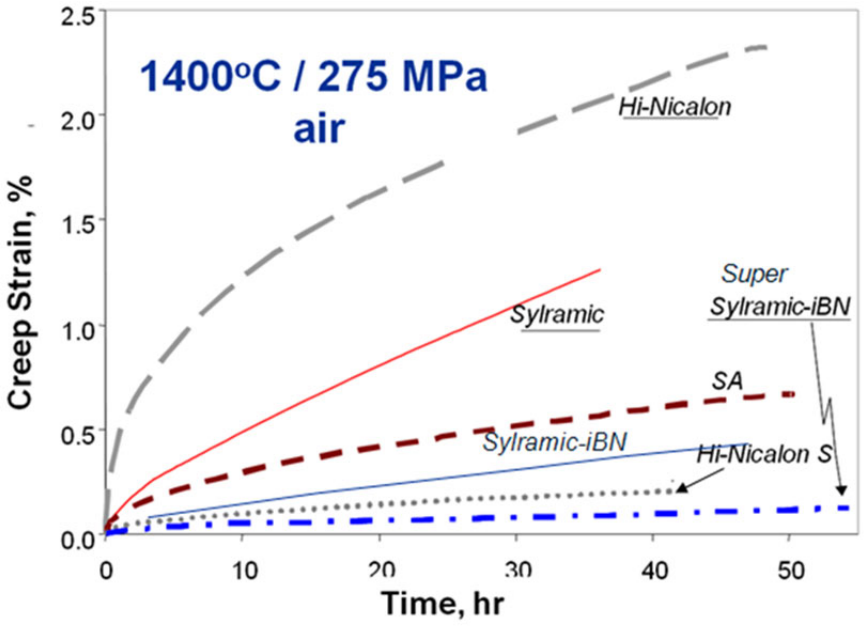

Figure 1.—Creep strain behavior of various SiC fiber types in single fiber form (Ref. 17).

Here (**C**) is a composition-dependent diffusion constant; (**d**) is average fiber grain size; (**Q**) is the activation energy controlling steady-state creep; and (**R**) is the universal gas constant (8.314 J/mol.K). Thus for a given applied stress and temperature, Equation (1) indicates that the HNS fiber secondary creep strain could possibly be reduced by an order of magnitude simply by increasing its grain size from 20 to 200 nm. But due to decomposition of the silicon-oxycarbide phase pre-existent in this fiber, heat treatments above ~1600 °C, although increasing the HNS fiber grain size and improving its creep resistance, causes an undesirable loss in fiber strength (Ref. 15).

Besides limiting grain size, the oxide-based phase in the HNS fiber also gives rise to an undesirable large primary creep stage for this fiber type (Ref. 17). A convenient method for seeing this effect is by examining Table 2, which compares the parameter (**m)** measured in a Bend Stress Relaxation (BSR) test (Ref. 19) after 1 hr exposure at various temperatures in argon. The listed (**m**) data are not only for the HNS fiber, but also for two other high-performance SiC fiber types that possess less oxygen content after fabrication (Ref. 20). Since stress relaxation is caused by creep, the following equation for (**m)** values >0.5 is a good approximation for a fiber's primary creep strain ($\boldsymbol{\varepsilon_p}$) (Ref. 17):

$$\varepsilon_p = \varepsilon_e\left[(1/m) - 1\right] \tag{2}$$

Here $\varepsilon_e = \sigma/E$ = elastic strain on the fiber. Thus one can see in Table 2 that the as-produced HNS fiber shows primary creep as low as 1100 °C where its (**m**) value begins to fall below unity after only 1 hr; whereas the other two fiber types do not show this behavior until higher temperatures. It is believed that this creep is caused by grain boundary sliding accommodated by the low viscosity silicon-oxycarbide phase within the HNS boundaries (Ref. 21). Furthermore, on the practical side, one can see by Equation (2) and Table 2 that the HNS primary strain is approximately equal to its elastic strain after only 1 hr at ~1450 °C (**m** = 0.5). This implies a 50 percent loss in fiber stiffness or modulus in just that 1 hr period which, depending on the matrix type, could cause a stress overload on the matrix, causing it to crack. Thus based on the observed limitations of the HNS fiber, in order to achieve SiC/SiC composites with improved structural performance and temperature capability, *it is important to seek SiC fibers with little or no low-viscosity phases in the grain boundaries and with average grain sizes up to ~500 nm*. The guideline for little or no low-viscosity phases in the grain boundaries is also important for creep of the SiC matrix.

One proven approach for obtaining SiC fibers with greater temperature capability than the HNS fiber is to allow by thermal treatment the silicon-oxycarbide phases that are typically created during fiber fabrication to decompose as gases, resulting in a weak SiC fiber with fine-sized pores. Then by incorporating sintering aids in the fiber pre-ceramic polymer (Refs. 9 and 22) or by gaseous infiltration of the pores with sintering aids after decomposition of a SiCO fiber (Refs. 23 and 24), the pores are then removed by sintering treatments to 1800 °C and above. This approach typically results in high-density near-stoichiometric SiC fibers with little remaining oxide phases and with average grain sizes greater than 100 nm, two important microstructural conditions not available in the HNS fiber. Also this sintering approach has the major advantage of producing strong fibers at very high production temperatures, which can significantly open the temperature window for CMC fabrication and service without experiencing microstructural instabilities in the fiber reinforcement.

TABLE 2.—AVERAGE BSR (M) VALUES FOR SINGLE NEAR-STOICHIOMETRIC SiC-BASED FIBERS MEASURED AFTER 1-HR EXPOSURE IN ARGON AT VARIOUS TEMPERATURES (REFS. 19 AND 20)

Fiber type	1100 °C	1200 °C	1300 °C	1400 °C	1500 °C
Tyranno SA3	----	0.90	0.74	0.45	----
Hi-Nicalon Type-S	0.96	0.89	0.83	0.64	0.40
Sylramic-iBN	1.00	0.97	0.91	0.84	0.74

Today two commercial SiC fiber types are using this sintering approach: the “Tyranno SA3” fiber from UBE Industries where an aluminum-based sintering aid is incorporated into a SiC-yielding pre-ceramic polymer (Ref. 9); and the “Sylramic” fiber originally produced by Dow Corning and now by ATK-COI Ceramics in San Diego, California, where a boron-based sintering aid is infiltrated into the pores of a decomposed SiCO precursor fiber (Ref. 24). Table 1 lists some key as-produced properties of these two fiber types, and Figure 1 compares the tensile creep behavior of these fibers against HNS under the same test conditions of 1400 °C, 270 MPa, and laboratory air. As can be seen, although the Tyranno SA and Sylramic fibers are near-stoichiometric with high strength and high thermal conductivity, their high-temperature tensile creep behavior is worse than that of the HNS fiber. This less than optimum creep behavior can be attributed to the aluminum and boron-based sintering aids that still remain in the grain boundaries of the as-produced fibers, thereby enhancing the rate of grain boundary sliding. Realizing this issue, NASA developed high-temperature thermal treatments in selected environments to remove or alter the sintering aids in the as-produced fibers. It was determined that whereas the grains grew and creep-resistance improved, the low tensile strength of the as-produced Tyranno SA fibers degraded further with high-temperature thermal treatment. On the other hand, the boron in the Sylramic fiber sintering aids could be removed in both nitrogen and argon atmospheres with retention of high tensile strength (~3 GPa), and with significant improvement in fiber creep resistance (Ref. 25). When treated in one atmosphere of high-purity nitrogen, the resulting fiber has been labeled “Sylramic-iBN” because as the boron is removed from the as-produced Sylramic fiber, a thin protective in-situ grown BN (iBN) coating is formed with uniform thickness on the circumference of each fiber, even those in tight contact with its neighbors within a woven tow (Ref. 6). When treated in high-purity nitrogen above one atmosphere, fibers with even more creep resistance have been produced and have been labeled “Super Sylramic-iBN” (Ref. 14). Key properties and the improved tensile creep behavior of the Sylramic-iBN SiC fiber (hereafter iBN fiber) and the Super Sylramic-iBN fiber over their precursor Sylramic fiber are shown in Table 1 and Figure 1, respectively.

It is interesting to note in Figure 1 that under creep testing at 1400 °C, the iBN fiber is slightly less creep resistant than the HNS fiber; whereas the Super iBN fiber is slightly more creep resistant. By Equation (1), if grain size were the only difference, this result would be unexpected since the average grain size of both iBN fibers is at least an order of magnitude larger than that of the HNS fiber. On the other hand, the bend stress relaxation (BSR) results of Table 2 show a significant improvement in creep resistance in the primary stage for the iBN fiber over the HNS fiber. Recent NASA studies attribute these apparently contradicting results to the fact that after sintering, the Sylramic as well as the Tyranno SA fibers display a cross-sectional microstructure consisting of large grains in a thin shell at the fiber surface and a core region consisting of smaller grains and fine-size pores (Ref. 26). It would appear that the shell region is created prior to or during sintering by the concentration near the fiber surfaces of the aids responsible for grain growth. Thus, similar to the fiber-matrix creep conditions described above for Case A, at high temperatures the more creep-prone inner region within the fibers will shed its load to the more creep-resistant shell region, which only occupies ~30 percent of the total cross-sectional area. As such, the stress on the shell can be as much as ~3 times larger than that on the HNS fiber, which contains a more uniform cross-section (Ref. 26). Then by Equation (1), the tensile steady-state creep rate for the iBN would be ~33 times greater than the HNS fiber at the same grain size. Thus, the perceived tensile creep advantage of a larger grain size for the iBN fiber is effectively lost by its nonuniform cross-section. Also, it follows that since the BSR test primarily samples the creep-resistant shell region, the BSR data for the iBN fiber would be expected to show much better creep-resistant behavior than that of the HNS fiber.

Because it can be more conveniently produced without the need for high-pressure nitrogen, the iBN fiber in contrast to the Super Sylramic-iBN fiber has gone beyond the developmental stage to commercial availability as multifilament tows. It also has been available for nearly a decade to be employed in SiC/SiC CMC panels as 2D-woven fabric for the NRMI fabrication route and for 3D-woven pre-forms using CVI-MI and other matrix infiltration approaches. This has allowed a direct property comparison between CMC reinforced with the HNS and iBN fibers. For example, during creep-rupture tests at 1315 °C in laboratory air (Ref. 27), the HNS CMC showed a significant initial increase in creep strain in

comparison to the iBN CMC when the applied on-axis stress increased from 103 to 138 MPa. Each CMC type was fabricated by the NRMI route with 2D-woven balanced fabric and ~18 percent fiber content in the loading direction. It would appear that this behavior is caused by a lower MCS for the HNS CMC and/or by the larger primary creep stage of the HNS fiber. This later mechanism is supported by the BSR data in Table 2 that shows after 1 hr at 1300 °C, the creep of the iBN fiber is much less than that of the HNS fiber. As a result, on initial CMC loading, the primary creep for the HNS fiber allowed the NRMI matrix to exceed its micro-cracking strain limit of ~0.05 percent (CMC modulus ~265 GPa) before it can stress relax and shift most of its load to the fiber. Thus it would appear that the higher HNS CMC creep behavior at 138 MPa is indicative of local matrix cracking, leaving the crack bridging fibers to carry much higher stress levels they would experience in an uncracked CMC (Ref. 4). On the other hand, matrix cracking was probably not occurring in the iBN CMC, allowing these fibers to creep at lower stress levels and thus providing a CMC with reduced creep.

For MI CMC specimens at low stresses with no matrix cracking, steady state creep behavior can be predicted well by NASA's analytical creep models determined from the creep behavior of single HNS and iBN fibers by assuming that all the fibers after long times are carrying the entire CMC load, (Ref. 17). This is not only true for CMC fabricated by the NMI route, but also for CMC fabricated with HNS fibers by the RMI route (Ref. 28). This implies that at least in laboratory air, the rupture life of these CMC should be predictable by understanding the *intrinsic rupture characteristics* of these two fiber types. However, although these characteristics have been measured for single HNS and iBN fibers as a function of stress and temperature (Ref. 29), one should realize that the fiber conditions within a cracked CMC during high-temperature application could be considerably different than those employed during simple creep-rupture testing of single fibers. For example, the condition of tensile stress being held constant both in time and along the fiber length will probably not exist within a CMC due to fiber curvature induced by the fiber architecture and to the typical occurrence of CMC matrix micro-cracking, where fiber stresses are highest within the matrix cracks and then drop off within the intact segments of the matrix. Also under these CMC conditions, not only is fiber gauge length considerably smaller than the 25 or 100 mm length typically used for single-fiber creep-rupture testing, but also rupture is controlled by bundles of fibers rather than single fibers. In addition, if the testing environment plays a role on fiber rupture, testing in laboratory air may give different results than testing within a given composite application environment. For this reason, NASA has found it more practically useful to understand and empirically model the general rupture characteristics of various fiber types by examining the rupture characteristics of CMC specimens in which the reinforcing fibers are (1) loaded on axis with the primary fiber direction at a known fiber content, (2) are essentially straight in the loading direction, and (3) the CMC matrix carries little or no load because it is more creep prone than the fiber. The results of this approach are discussed in Section 4.5.

In summary, when compared to the HNS fiber, the iBN SiC fiber is more thermally stable due to its higher production temperature, thereby allowing higher SiC/SiC fabrication and service temperatures without fiber tensile strength degradation. Its higher production temperature also results in lower oxygen content for a reduced primary creep stage, plus larger grains for much improved thermal conductivity and the potential for improved creep if its microstructure can be made more uniform in grain size distribution. In addition, the in-situ grown BN layer provides more environmental resistance than the carbon-rich or non-carbon-rich surfaces of the HNS fiber as well as the CVI produced BN-based interfacial coatings that cannot cover the full fiber surface in high fiber fraction CMC. However, beyond its nonuniform microstructure, certain other issues are currently limiting optimum application of the iBN fiber. For example, its larger grain sizes in comparison to those of the HNS fiber typically result in rougher fiber surfaces, which although beneficial for high interfacial stress and tight crack opening, can be detrimental in that they can cause fiber-fiber abrasion and fiber fracture when multifiber tows are woven or braided into complex pre-forms. Also, as will be discussed in Section 4.5, the larger grains appear to reduce the ultimate creep strains that the fiber can reach without rupture. In addition, there is the general increase in the acquisition costs for sintered fibers that typically accompanies their higher production temperatures.

Finally, the Sylramic precursor fibers for the iBN SiC fibers are currently produced commercially by a combination of batch and continuous processing, which limits their availability in sufficient quantities for production-ready components.

4.2 Advances in Interfacial Fiber Coatings

Although the SiC fiber controls many of the key structural properties of SiC/SiC composite systems, the other key composite constituents also need to be optimized in composition and geometry for durable component use. For example, in early SiC/SiC composites, the preferred interfacial fiber coating composition was carbon as formed by the CVI process. However, under certain conditions, it is likely that these coatings will be exposed to aggressive environmental conditions, for example within a matrix crack, but also at free or cut CMC edges. For this latter condition, NASA has shown that under the conditions of high-velocity combustion gases, these carbon-based coatings can be quickly removed by oxidation, and that this removal could occur throughout the composite because of fiber-fiber contact (Refs. 16 and 30). Working within the EPM program, NASA has demonstrated that a more stable coating would be based on a CVI-produced silicon-doped BN composition. This is the case because BN is not only structurally weak for crack deflection, but instead of forming a volatile gas upon oxidation, it forms in the presence of silicon a nonfugitive product (borosilicate glass), thereby preventing further oxygen ingress into the composite.

Although silicon-doped BN coatings have proven useful for CMC with free or cut CMC edges, if stress-induced matrix crack deflection occurs at the fiber surface rather than on the outside of the interfacial coating, the environment entering the matrix crack could reach and degrade the SiC fiber. To address this concern, NASA developed CMC thermal treatment processes that would allow the BN coating to shrink towards the fiber surface and debond from the matrix, thereby assuring crack deflection to occur on the outside of the fiber-protective BN coating (Ref. 31). Even though the interphase coating remains attached to the fiber and debonded from the matrix, load transfer between the fibers and matrix is still maintained within complex-shaped fiber architectures that allow the interfacial coating to mechanically slide against the matrix during the application of stress. In comparison to multilayer concepts for interfacial coatings, this “outside debonding” approach avoids the fabrication of complex interphase compositions and structures, does not rely on uncertain microstructural conditions for matrix crack deflection outside of the interphase, and provides a more reliable approach for retention of the total interphase on the fiber surface. As mentioned earlier, this oxidation protective scheme is further enhanced by use of the Sylramic-iBN fibers that also have a thin in-situ grown environmentally-resistant BN coating on their surfaces. As a result of outside debonding, a SiC/SiC system with 2D fiber architectures will typically display a slightly lower thru-thickness thermal conductivity due to partial loss of matrix thermal contact with the fibers. However, NASA has shown that this effect can be mitigated by the use of 3D architectures as discussed in the next section.

4.3 Advances in SiC Fiber Architectures

As with any composite component reinforced by high-performance continuous fibers, one of the primary requirements is to design the fiber architectures to provide sufficient fiber content in those directions that are structurally loaded during component service in order that the fiber-controlled structural properties of the component, such as MCS, will be sufficient to allow it to survive without failure during its required lifetime. For SiC/SiC components, life-limiting failure mechanisms are generally identified with (a) thru-thickness matrix cracking under in-plane tensile loading, and (b) delamination cracking under thru-thickness tensile loading. In the first case, thru-thickness cracking will allow the service environment to reach and degrade the crack-bridging fibers within time periods typically less than the required component lifetime. For aero-propulsion components, this situation would apply, for example, to the walls of pressure-cooled airfoils and to centrifugally loaded blades (Ref. 32). In the second case, delamination cracking can increase the thermal stresses and wall temperatures for internally cooled turbine components, increasing the risk of wall spallation and other component damage. Thus the

general fiber architecture goals for SiC/SiC components are to achieve a starting pre-form with (1) a shape as close as possible to the final component shape and (2) a total fiber content as high as possible, and (3) a judicious splitting of this total fiber content in-plane, thru-thickness, and locally to allow the CMC directional MCS properties to sufficiently exceed the component service stresses. Furthermore, if the fiber is thermally conductive, it will aid in increasing the CMC directional thermal conductivities, thereby reducing service-related thermal stresses in these directions.

When the current 2D fiber architecture designs of the NRMI and RMI fabrication routes are compared to the above goals, certain deficiencies can be observed. For example, regarding CMC in-plane properties, although the 2D woven fabric approach of the NRMI fabrication route (and other routes that use 2D fabric) have reached total fiber contents as high as 50 percent, their in-plane fibers are not straight. Depending on the weave pattern, the effective on-axis fiber modulus and strength will be less than those of straight fibers, which in turn will debit CMC thru-thickness matrix cracking strength (MCS), ultimate tensile strength (UTS), and rupture strength (to be discussed). In the case of the RMI or prepreg fabrication route, although the in-plane fibers are effectively straight, total fiber contents are not high (<30 percent) due to the need to individually coat almost every fiber with a thick interphase. Thus all fiber-controlled properties are less than optimum for the RMI route.

Regarding CMC thru-thickness properties, it is found that as the multiply 2D-woven fabric of for the NRMI route is compressed in tooling prior to interphase deposition, the resulting CMC thru-thickness tensile strength and thermal conductivity will generally increase. This effect is primarily due to increased fiber-fiber contact and intermingling or “nesting” of the fiber tows. But as might be expected, this nesting results in less opportunity to achieve uniform CVI-produced interfacial coatings on all the fiber surfaces in a tow or thru the thickness, plus increased mechanical degradation of the fibers and CMC in-plane strength properties. Whereas the NRMI route relies on increasing fabric nesting to improve the CMC thru-thickness or Z-direction properties, the RMI route relies on its low total fiber content to allow the dense SiC-based matrix between the fibers to provide monolithic-like thru-thickness tensile strength. For both the NRMI and RMI routes, it is difficult to obtain reproducible CMC thru-thickness properties due to local microstructural variances. This results in large scatter, for example, in the thru-thickness or Z-direction properties, which in turn results in significantly low thru-thickness tensile strength allowables (<20 MPa) for current SiC/SiC components. Finally, both fabrication routes rely on the lay-up of finite-sized 2D plies, which means that for components with continuous surfaces, such as combustor liners and airfoils, there must be regions where the plies terminate and fiber reinforcement is absent. Thus unless the ply ends are intermingled in some judicious manner, or the ply ends are located in low stress regions, there can be a significant knockdown in component strength properties at these locations (Ref. 33).

Realizing the general architecture goals and the deficiencies of the two MI fabrication routes, NASA in recent years has been examining SiC/SiC CMC panels primarily consisting of multiple types of 3D-woven pre-forms with thru-thickness fiber reinforcement. These types range from simple 2.5D-woven to more complex 3D-orthogonal architectures (Refs. 34 and 37). In most cases, iBN SiC fiber tows have been used as the in-plane warp and fill stuffers, and the interfacial coatings and matrices were formed by those used in the NRMI fabrication route. For the warp weaver or thru-thickness fibers, due to their high stiffness and tendency to fracture under high bend angles, iBN fibers were only used for preforms with low-angle thru-thickness tows; whereas low-stiffness low-performance SiC-based “ZMI” fibers were used for the high-angle 3D-orthogonal pre-forms. Table 3 lists the key room temperature in-plane and thru-thickness properties for some 2.5D and 3D SiC/SiC panels and compares them with panels fabricated by the standard NRMI route using the lay-up of 2D-woven iBN fabric (NASA N24A SiC/SiC). For the Table 3 panels, the in-plane iBN stuffer tows were nearly straight with total fiber contents of ~36 percent, and were nearly balanced at ~18 percent in each of the warp and fill directions or were un-balanced at ~10 percent in the warp and ~25 percent in the fill direction. The indicated test data were measured in-plane in the fill or Y direction, as well as in the thru-thickness or Z direction.

TABLE 3.—TYPICAL DIRECTIONAL STRENGTH AND THERMAL CONDUCTIVITY PROPERTIES OF SiC/SiC PANELS WITH VARIOUS WOVEN FIBER ARCHITECTURES[a]

SiC/SiC Fiber architecture		Fiber content, percent			20 °C CMC directional strengths, MPA			CMC directional thermal conductivity, W/m.K			Ref.
					Y		Z	X	Z	Z 1400 °C	
		X	Y	Z	MCS	UTS	UTS	20 °C	20 °C		
A	2D fabric	18	18	0	180	460	15	50	25	18	6, 32
B	2.5D	17	19	3	140	360	28	--	50	25	35, 36
C	3D Orthogonal	18	17	<5	120	320	--	--	--	--	37
D	3D Orth-Unbal	10	25	<5	240	600	--	--	--	--	37

[a]X, Y stuffer fibers = Sylramic-iBN fiber; Matrix fabrication = CVI-MI;
2.5D Z weaver = Sylramic-iBN fiber; 3D Z weaver = ZMI SiC Fiber

Table 3 shows that for the NRMI fabrication route, significant advances can be achieved in SiC/SiC CMC structural and thermal properties by the use of 3D-woven pre-forms rather than by the current 2D-woven fabric lay-up approach. For example, when the 2D-woven Panel A is compared against the 2.5D-woven Panel B, although a small knock-down occurred for the in-plane strengths, one can see a doubling in the Z-direction properties of thru-thickness tensile strength (Z-UTS) and thermal conductivity (Z-TC) at room temperature, but also a significant increase in Z-TC at 1400 °C (extrapolated). Indeed this latter Z-TC value of 25 W/m.K may be the highest ever measured at high temperature for SiC/SiC panels. These improvements were achieved with only ~3 percent iBN fibers in the Z direction, so that further improvements should be expected with higher Z-fiber content. Whereas the Z-UTS improvement can be explained by the use of strong iBN fibers, the improvement in Z-TC was probably due in part to the high conductivity of these fibers and in part to the fact that weaver fibers probably allowed better infiltration channels for the NRMI matrix.

Then when one compares Panel A with the balanced 3D-orthogonal Panel C, one finds a further decrease in in-plane strengths, even though the Y-stuffer fibers in Panel C are straighter than those in Panel A. This degradation in the warp and fill stuffers of Panel C may have been caused by excessive abrasion with the ZMI weaver fibers and/or to reaction with these fibers during high-temperature CMC fabrication. Finally, when one compares the balanced 3D-orthogonal Panel C with the un-balanced 3D-orthogonal Panel D, one sees an approximate doubling of the in-plane Y-direction strengths, even though the fiber content in this direction only increased from ~18 to 25 percent. Thus, although these results are preliminary, one might conclude that the demonstrated Z-direction property benefits of thru-thickness fibers need not necessarily exclude improvement at the same time of the in-plane properties, provided one makes a judicious choice of the SiC fiber and its 3D architecture.

Beyond improved thru-thickness strength and conductivity, NASA has shown that the 2.5D-woven architectures with iBN fibers also provide SiC/SiC CMC with improved delamination resistance and impact resistance in comparison to 2D architectures (Ref. 38). As discussed above, another potential advantage for 3D architectures can be enhanced matrix infiltration down the weaver fibers, resulting in reduced matrix porosity. Furthermore, the possibility may exist that the automation aspects of 3D weaving or braiding will result in reduced manufacturing costs and reduced scatter in composite properties by eliminating the human element that is typically involved in 2D fabric and tape lay-up techniques. However, for the highest temperature SiC/SiC components, sintered SiC fibers, such as the iBN and Tyranno SA fibers, are near-stoichiometric in composition with large nano-sized grains, resulting in high bending stiffness and rough fiber surfaces leading to poor abrasion resistance. As described for the panels in Table 3, these issues can enhance the probability of fiber fracture during 3D pre-forming and thus limit the available 3D-woven architectural designs and thru-thickness fiber fractions. Nevertheless, NASA has recently demonstrated with a commercial textile processing vendor that complex 3D-woven pre-forms for SiC/SiC panels as well as for SiC/SiC turbine airfoils can be fabricated using polymer-based “serving” fiber tows that are wound around sintered SiC fiber tows prior to weaving, thereby significantly reducing their abrasion issues (Ref. 39). In subsequent CMC processing, these fibers will decompose leaving a negligible carbon char, which should be of little issue for the key

CMC properties. Another potential approach developed at NASA for complex-shaped components is to first form 3D pre-forms with simpler shapes that are close to those required by the component, but do not contain the extreme bends that can cause fiber fracture. Then one can heat treat the architecture while applying continuous or discrete levels of pressure to creep-form the fibers without fracturing them into the tighter bends required by the component shape. NASA has demonstrated that this can be done at the same time as the iBN treatment with minimal loss in fiber strength (Ref. 25).

4.4 Advances in SiC-Based Matrices

Since the free silicon in the NRMI and RMI matrices limits their long-term SiC/SiC CMC upper use temperatures to less than 1300 °C, NASA and the U.S. Air Force have recently been researching and developing SiC/SiC systems by using alternate matrix infiltration processes into stacked 2D-fabric pre-forms that result in SiC compositions that are effectively silicon-free. To date, three such infiltration processes have been extensively evaluated (Ref. 34): (1) CVI processing where SiC deposition is continued as long as possible to fill the porosity within an interface-coated 3D pre-form (Full CVI approach); (2) polymer-infiltration and pyrolysis (Full PIP approach) in which multiple infiltration cycles are performed, each consisting of infiltration of a SiC-yielding polymer into the remaining 3D pre-form porosity, followed by polymer decomposition at high temperatures into crystalline SiC particulates; and (3) a hybrid of these two processes, where typically the CVI approach is first used for partial filling of the pre-form porosity, and then the remaining porosity is filled as much as possible by subsequent multiple PIP cycles (CVI-PIP approach). Although achieving the goal of an effectively silicon-free SiC matrix, each of these three processes have various advantages and issues that may or may not limit their application for higher temperature SiC/SiC components.

In terms of advantages, the Full CVI method for matrix infiltration is amenable to the fabrication of SiC/SiC components having irregular, large, and complex shapes with near-net shape capability. High temperature properties are generally good because high purity matrices with controlled microstructures can be obtained. Aside from trapped porosity (10 to 15 vol%), this approach typically results in a SiC matrix material with high thermal conductivity and high creep resistance in multiple directions. Also CVI is carried out at relatively low temperatures (<1000 °C), so that there is little risk of fiber damage. In addition, the fiber-matrix interphase can be tailored by pre-coating the fiber preform during an initial CVI step using different reagents, but the *same* reactor. However, one of the major limitations of the Full CVI method is the long deposition times needed for the densification process (typically greater than 100 hr). This raises the cost of the component fabrication in comparison to processes that require much shorter times to complete the matrix infiltration. Furthermore, although the CVI matrix initially forms fairly uniformly within the fiber tows and then on the surface of the tows, as deposition continues nonuniform regions of matrix with large and sharp pores typically form between the tows due to their separation and due to their depth within the CMC thickness. Because of their size and irregular shapes, these trapped pores reduce the CMC MCS in multiple directions. Thus it is not possible to obtain fully dense matrices using the Full CVI approach. In addition, the typical presence of residual closed porosity may shorten the useful life of the CMC component particularly after matrix cracking in an oxidizing environment. Finally, in relation to fully dense CMC, the trapped or closed porosity will not allow CMC with maximum thermal conductivity.

Regarding the Full PIP approach, its main advantage is its use of methods typically employed and well established in the fabrication of polymer matrix composites. Thus in contrast to the Full CVI approach, the size of CMC components is not limited by the size of the CVI reactor. However, one of its main drawbacks is the long processing times and repeated infiltration/pyrolysis cycles in order to obtain sufficiently high matrix density. Due to polymer shrinkage during pyrolysis, another drawback is that matrix micro-cracking generally results within the CMC in the form of fine cracks between the crystallized particulates. Re-infiltration fills these cracks to some degree, but matrix cracking strength and thermal conductivity in multiple directions generally remain low in comparison with the Full CVI approach. Finally, due to oxygen in the polymer and also multiple cycles from room to high temperature,

oxygen is typically picked up within the fine cracks, which then can attack the interphase and fibers unless oxygen getters are also introduced into the matrix (Ref. 34).

For recent research and development studies aimed at silicon-free matrices, NASA has been emphasizing the CVI-PIP hybrid approach because it avoids to a large degree the drawbacks of the Full CVI and Full PIP approaches while incorporating some of their advantages. For example, just as in the NRMI fabrication route, only partial CVI deposition is utilized, thereby affording much shorter deposition times and reduced risk of large inter-tow pores, while retaining a partial SiC matrix with high strength, high creep-resistance, and high thermal conductivity in multiple directions. In addition, the partial CVI SiC matrix provides environmental protection for the interphase and fibers during subsequent matrix infiltration processes. Filling the remaining matrix by the PIP approach allows the introduction of high conductivity SiC particulates without the concern of oxygen pick-up during multiple PIP cycles. Although fine cracks will still exist between the particulates, they are much finer than those that form during cracking of the CVI matrix so that they can seal much more rapidly in high-temperature oxidizing environment. Nevertheless, although the hybrid approach has these multiple advantages, it like the other approaches does not as yet yield matrices with zero or near-zero porosity.

Table 4 compares some key in-plane and thru-thickness properties at 20 and 1450 °C for SiC/SiC CMC panels fabricated with matrices infiltrated by the CVI-MI, Full CVI, Full PIP, and hybrid CVI-PIP approaches. The first set of panels employed 2D-woven iBN fabric; while the second set employed 2.5D woven iBN tows. To achieve maximum performance in terms of reduced matrix defects and increased matrix creep resistance and thermal conductivity, all the panels with silicon-free matrices were post-processed at NASA by annealing treatments above 1500 °C (Refs. 6 and 35). Examining Table 4, one can see that currently all the indicated processes for Si-free matrices do not achieve the low ~5 percent porosity of the CVI-MI approach. The high porosity levels of ~15 percent typically result in lower matrix cracking strengths depending on fiber content and the character of the porosity, and in variable ultimate strengths, also depending on fiber content and possibly on the resistance of the iBN fibers to attack during CMC processing and post treatment. One approach to acquire better information about the matrix structural quality is to test the CMC in an off-axis direction where the matrix carries more of the CMC load. Thus when tested at 45° to the balanced X and Y directions, Table 4 shows a significant knockdown in the X/Y-UTS for the Full PIP panel, indicating that this matrix approach does not have the structural quality provided by the partial CVI or Full CVI approaches. On the other hand, the Full PIP displays a relatively high Z-UTS. As previously described, this is caused primarily by increased fabric compression and nesting of the fiber tows between fabric plies. Furthermore, due to the fine cracks, the Full PIP panel does not compare in thermal conductivity with the other matrix approaches. This low Z-TC property is probably due in part to the need for boron-based oxygen getters purposely incorporated in the matrix to avoid the effects of oxygen pickup during the multiple PIP cycles (Ref. 34).

TABLE 4.—TYPICAL EFFECTS OF VARIOUS MATRIX INFILTRATION APPROACHES ON DIRECTIONAL STRENGTH AND THERMAL CONDUCTIVITY PROPERTIES OF SiC/SiC PANELS[a]

SiC/SiC Matrix approach	Y Fiber, percent	Matrix		20 °C CMC directional strengths, MPa				Z thermal conductivity, W/m.K		Ref.
		~Free Silicon, percent	~Total porosity, percent	Y MCS	Y UTS	XY UTS	Z UTS	20 °C	1400 °C	
	2D-woven Sylramic-iBN fabric									
CVI-MI	18	13	5	180	460	240	15	25	18	6, 32
Full CVI	18	0	15	120	350	---	7	28	8	34, 35
Full PIP	21	0	<15	140	400	<100	23	8	5	34, 32
CVI-PIP	18	0	14	150	360	---	10	28	10	34, 35
	2.5D-woven Sylramic-iBN Tow									
CVI-MI	18	13	5	140	360	---	28	50	25	36
CVI-PIP	18	0	14	130	380	---	24	45	22	36

[a]All silicon-free SiC/SiC CMC were post treated above 1500 °C

Regarding the hybrid CVI-PIP approach, although it can provide SiC/SiC that can operate at higher temperatures, Table 4 shows that with conventional 2D-woven architectures, it does not as yet provide comparable properties with CMC fabricated with the CVI-MI matrix approach. As might be expected from their high residual porosity, the 2D-woven CVI-PIP panels show a small knockdown in Y-MCS and Z-UTS, as well as high temperature Z-TC, but their values are still higher than those of the Full CVI panels. Nevertheless, as also shown in Table 4, when the hybrid matrix approach is combined with a 2.5D-woven architecture, the resulting panels, while still retaining a small deficient in in-plane properties, display significant improvement in Z-UTS and Z-TC in comparison to those fabricated by the 2D-woven route and CVI-MI matrix. Thus if the porosity can be reduced and advanced 3D-architectures with iBN fibers are employed, the hybrid CVI-PIP matrix approach has the potential of not only displaying better structural and thermal properties than the current NRMI or CVI-MI route for SiC/SiC components, but also higher temperature structural capability as discussed in the following section.

4.5 Advances in SiC/SiC Microstructural Design Methods

As discussed above, of key importance for SiC/SiC component implementation in high-temperature applications is the ability to select the optimum constituents and their geometries so that the component microstructure has the intrinsic structural capability to achieve the required component life under its projected mechanical, aerodynamic, and thermal loads. For this selection process, a method often used for metals and ceramics is to perform stress-rupture tests in which a constant stress is applied to a material at a constant high temperature under laboratory conditions. The time for total material rupture is then recorded for various combinations of stress and temperature. One simple and convenient empirical approach for representing the data from these tests is by use of "Larson-Miller" (LM) plots. In these plots, master curves are generated for various materials, which describe the applied stress at rupture (material rupture strength) versus the time-temperature dependent parameter **q** given by

$$q \equiv T\left(\log t_r + D\right) \tag{3}$$

Here **T** (Kelvin) is the absolute temperature for the rupture test, $\mathbf{t_r}$ (hours) is the material rupture time, and **D** is a constant that best allows the rupture data at different temperatures to fall nearly on one master curve. The designer can then compare the rupture test results for prospective materials for an initial down-select of those materials that can best meet the component's service requirements. NASA has determined that this LM approach with **D = 22** can be effective method for SiC-based fibers (Ref. 29) and also for SiC/SiC CMC (Ref. 40), not only for showing the effects of various constituents and architectures on the structural life of various SiC/SiC CMC, but also for demonstrating the benefits of the recent constituent advances discussed above.

In Figure 2, the LM approach has been used to plot the in-plane rupture strength data for various SiC/SiC composites versus the time-temperature at which they failed by complete rupture (Ref. 40). All CMC were fabricated as panels with by the NRMI route and tested on-axis with one of the primary fiber directions (content of ~18 percent), and were reinforced with balanced 2D-woven 0/90-balanced five-harness satin (5HS) fabrics of different SiC fiber types as indicated by the different curves. Also included is the predicted curve if an NRMI CMC were fabricated in the same manner using the developmental Super Sylramic-iBN fiber. Thus all CMC contained free silicon so that their long term creep and rupture behaviors were effectively controlled by the reinforcing fiber tows under the total CMC load. In Figure 2, one can see that the LM approach appears to be a good empirical method for predicting SiC/SiC rupture life in that the rupture strength data for various fiber types not only fall consistently near one best fit curve for each type, but also the curves closely follow the creep ranking of the different SiC fiber types as measured on single fibers in Figure 1. Although the data for each fiber type show some scatter from its best fit curve, the curves can still be clearly distinguished from one another. It is envisioned that some of data scatter for a specific fiber type may be due to whether or not matrix cracking occurred during initial CMC loading. Also it should be realized that with the LM approach, the scatter in rupture time data is

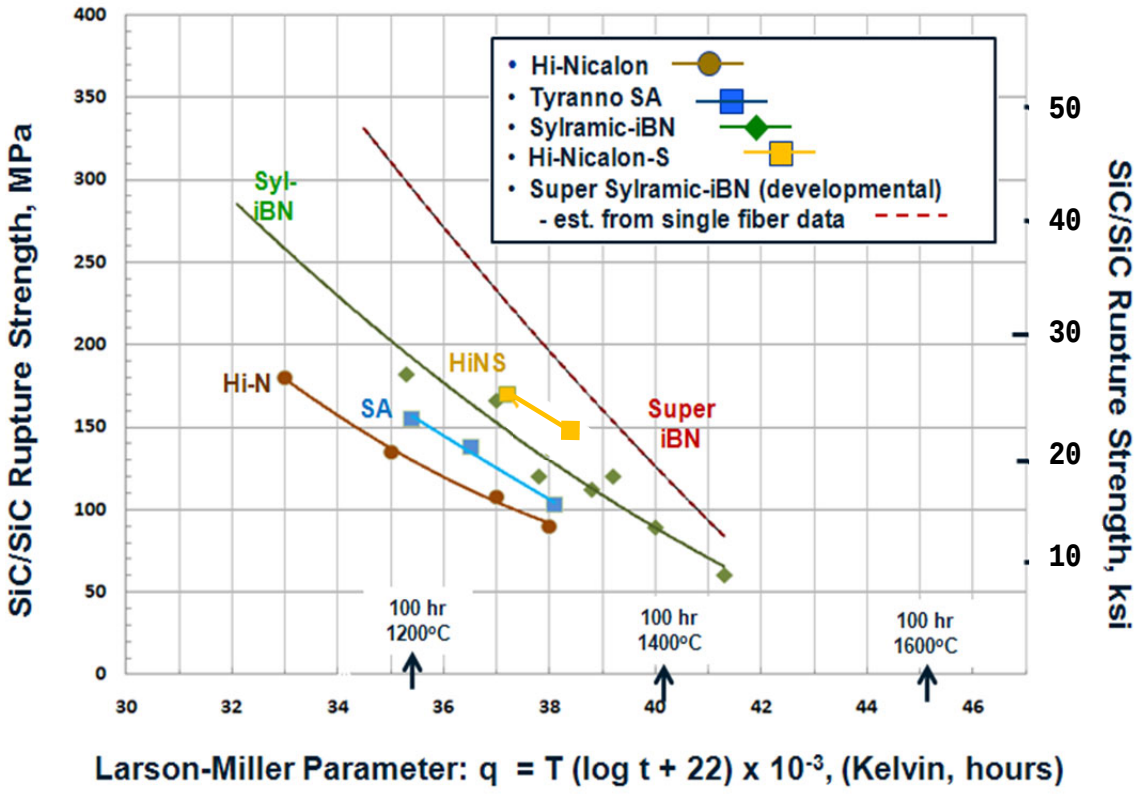

Figure 2.—Effects of SiC fiber type on on-axis rupture strength in air for SiC/SiC CMC with 2D-woven 0/90-balanced 5HS fabric, on-axis fiber content of ~18 percent, and CVI-MI matrix (Ref. 40).

greatly reduced by the time insensitivity of the LM (q) parameter. Thus the curves of Figure 2 are practically useful for understanding the projected rupture life of an NRMI-fabricated SiC/SiC component that needs to experience a maximum stress at a maximum temperature. For example, if the maximum on-axis stress for an un-cracked woven iBN/SiC component was 100 MPa, Figure 2 predicts a maximum **(q)** value of ~39400, which in turn would allow an intrinsic rupture life for the component of 100 hr at 1642 K (1369 °C), or 1000 hr at 1576 K (1303 °C).

Besides its practical implications, there are also various mechanistic conclusions one can draw from the Figure 2 results. For example, some of the data were taken at high enough CMC stress to initially crack the matrix, and yet the rupture strength data fall very close to the data where the CMC stresses did not cause initial matrix cracking. Thus, at least in laboratory air, the rupture mechanism for NRMI CMC appears to not be related to environmental attack, but to the fiber tows reaching a certain ultimate rupture strain during creep. For example, no matter the test conditions, the HNS CMC typically ruptures at ~0.6 percent total strain; whereas the iBN CMC ruptures at ~0.4 percent (Ref. 41). Thus in comparison to the iBN CMC, the slightly better rupture behavior of the HNS CMC in Figure 2 can be explained by its enhanced rupture strain, which in turn is probably related to its smaller grain size. It is also interesting to note that the rupture strains of the two fiber types are effectively equivalent to the ultimate fracture strains for their CMC in a room temperature fast-fracture test (Ref. 17).

The LM approach has also proved useful in understanding fiber architecture effects. For example, Figure 3 plots rupture strength data versus **(q)** data for a variety of different iBN-reinforced architectures within SiC/SiC panels fabricated with CVI-MI matrices (Ref. 40). The first set of data on the left reproduces the data in Figure 2 for NRMI-fabricated CMC reinforced by 2D-woven 5-harness satin fabric of iBN tows with on-axis content of ~18 percent. This curve is then projected to the right by assuming that if the same woven architecture could be produced with ~25 percent on-axis iBN fiber content, the final stress on the fiber would be reduced by a factor of 18/25 for the same CMC applied stress. Finally,

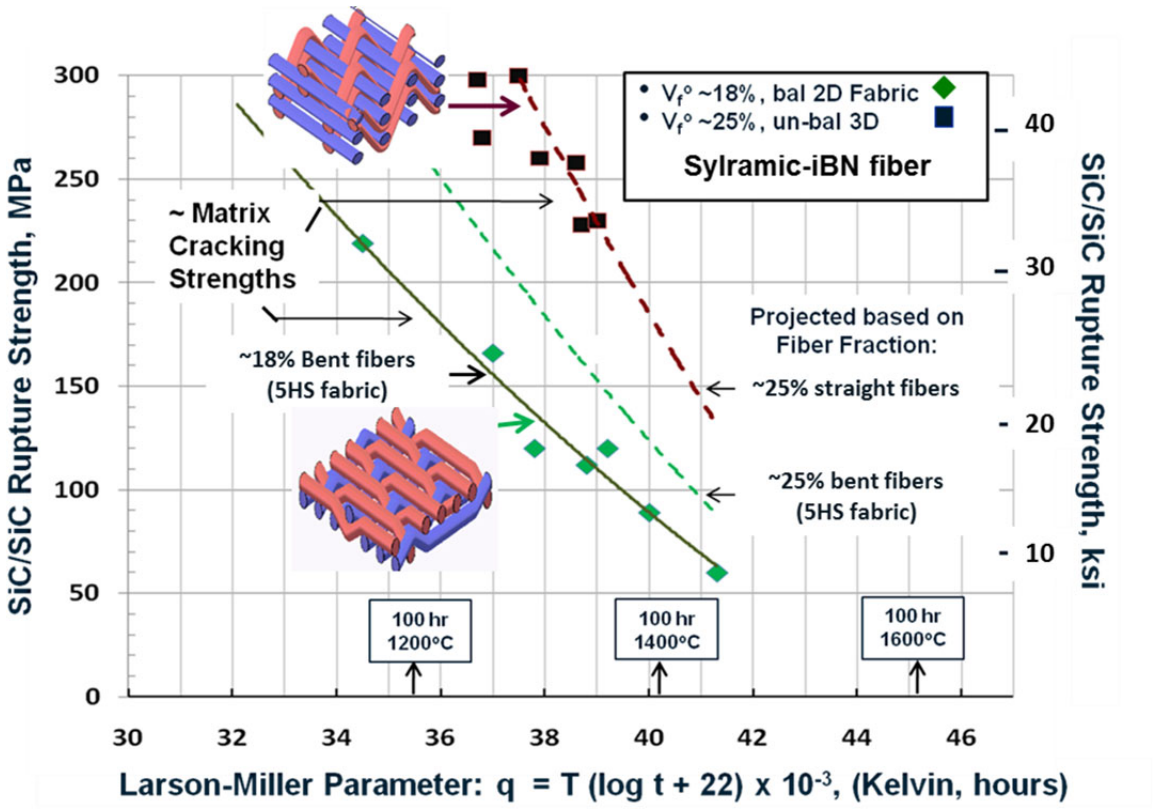

Figure 3.—Effects of fiber architecture on on-axis matrix cracking and rupture strength in air for SiC/SiC CMC with Sylramic-iBN woven tows and CVI-MI matrix (Ref. 40).

in the upper center of Figure 3 are the CMC rupture data (Ref. 41) measured in the fill direction for some of the 2.5D and 3D architectures described in Table 3. As previously indicated, in the fill direction the iBN tows were straight with an average fiber content of ~25 percent. When one compares this data set with the first set, one can see a significant improvement in CMC rupture strength for the same time-temperature test conditions. As indicated, this improvement is still much better than the middle curve which has the same fiber content, but incorporates bent fibers as a result of the woven fabric. Bottom line from Figure 3 is that the structural life of SiC/SiC components can be significantly improved by (1) increasing the fiber content in the key component directions and (2) assuring as much as possible that the fibers are in their as-produced straight condition.

Finally, one can use the LM approach in Figure 4 to understand the effects of different matrix infiltration approaches on SiC/SiC rupture behavior (Refs. 40 and 42). Here all CMC are again fabricated with 2D-woven 5-harness satin fabric of iBN tows, and the first data set on the left were fabricated by CVI-MI or the NRMI route. The next curve at higher (q) values is for CMC with Full PIP matrices, but with ~25 percent fiber content due enhanced fabric compression after lay-up. This data set is almost exactly 25/18 times the CVI-MI data set indicating that although containing no free silicon, the PIP matrix carries no long term load, leaving the fibers to again carry the entire CMC load. This effect can be attributed to little bonding between the PIP-generated SiC particulates caused by particle shrinkage during pyrolysis. Thus as previously discussed, the Full PIP matrix approach picks up its main advantage of higher fiber content in plane, but suffers in other key CMC properties. On the other hand, the post-annealed CMC with Full CVI matrix and ~18 percent fiber content does show improved behavior over the silicon-containing CVI-MI matrix with the same fiber content, suggesting that this creep-resistant matrix can carry some of the CMC load at temperatures where the CVI-MI and Full PIP matrices cannot. Finally, Figure 4 shows that although the post-annealed hybrid CVI-PIP approach does not have the CVI SiC content of the Full PIP, this could be an advantage by allowing more load to be put on the CVI SiC,

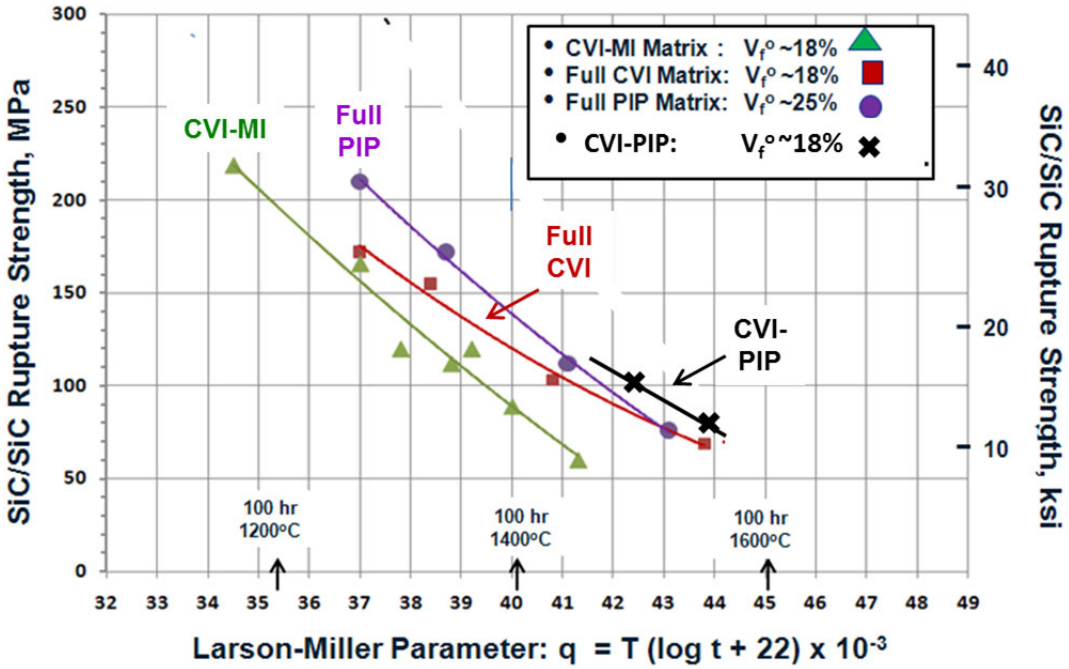

Figure 4.—Effects of matrix infiltration approach on on-axis rupture strength in air for SiC/SiC CMC with 2D-woven 0/90-balanced Sylramic-iBN fabric (Refs. 40 and 42).

causing it to creep at a rate closer to that of the fiber. In effect, this would be similar to increasing the fiber content. Thus for balanced 2D fiber architectures and post-annealed Si-free matrices, the hybrid CVI-PIP matrix approach currently yields the best high temperature SiC/SiC rupture behavior when compared to any other current approach (Ref. 42).

5.0 Current Microstructural Design Guidelines and Potential Service Issues for Higher Temperature SiC/SiC Components

The advancements described in this chapter offer a better theoretical and experimental understanding of the effects of various SiC-based constituent compositions and geometries on the key mechanical and thermal properties of SiC/SiC CMC. As such, they suggest the following general microstructural design guidelines for achieving a SiC/SiC component with high structural reliability and higher temperature capability than current SiC/SiC fabrication routes:

- Select (or develop) a polycrystalline small-diameter near-stoichiometric SiC fiber with average grain size between 200 to 500 nm, with grain boundaries free of such impurity elements as free silicon, free carbon, oxygen, boron, aluminum, and other elements that act as SiC sintering aids, and with a cross-sectional microstructure as uniform as possible in grain size and composition.
- Select (or develop) a fiber interfacial coating system that is compliant enough to deflect thru-thickness matrix cracks before reaching the fiber, is based on a composition that does not volatilize in an oxidative environment like carbon, and fully covers every fiber surface such as the iBN coating.
- Select, if possible, a fiber architecture that allows the final component shape to be textile formed, maximizes total fiber content in the component, allows sufficient fiber content in the key component stress directions, and eliminates or minimizes fiber curvature (straight fibers) in these directions.
- Select (or develop) a matrix process that yields a near-dense Si-free, tough, and SiC-based matrix that is highly thermally conductive and creeps slightly more than the fiber.

Although these guidelines may provide a SiC/SiC component with constituents that are intrinsically able to withstand quasi-static structural loads under uniform stress conditions, there are certain situations that can arise during component service that may still limit its performance and life and thus require further investigation. As discussed in Section 2.0, one such situation is related to creep in that, even if the creep mismatch between the fiber and matrix can be minimized, there will certainly be stress and temperature gradients within in the component leading to local amounts of differential creep strain, which in turn will result in local residual stress development that is not relieved at lower temperatures where the CMC behaves elastically (Ref. 5). These residual stresses can in turn reduce the local matrix cracking strength, so that during some follow-up situation, the weakened area could be unpredictably subject to a tensile stress that could exceed the local cracking strength. Hopefully the resulting cracking or damage will not alter affect the component performance or allow the service environment to enter and degrade the CMC microstructure. Clearly one approach for avoiding this situation is to only employ the component at temperatures and times where the CMC exhibits little or no creep. Thus if a certain high temperature performance is required for a SiC/SiC component, one should seek SiC fibers and matrices that display minimum long term creep at this temperature.

Another possible life-limiting issue is flaw or crack creation in the SiC/SiC component generated by unexpected mechanical and/or thermal shock. Mechanical shock, for example by foreign object impact, cannot only occur during component service, but also during general handling and assembly of the component. Currently, without sufficient engine experience, it is very difficult to predict the flaw severity that can arise from this effect or its degrading influence on component residual strength and structural life. For this reason, the general design approach should be to only seek SiC-based matrices that in their as-produced condition display high fracture toughness or high resistance to crack propagation from surface flaws, so that the as-produced matrix cracking strength of the as-produced component will be minimally compromised during service. Similar to mechanical shock, thermal shock can also lead to cracking, for example in a component wall as the colder side experiences an unexpectedly high tensile stress that is proportional to the CMC thru-thickness thermal conductivity. If cracking should occur under either shock situations, the reinforcing fibers will bridge the cracks providing they have sufficient tensile strength and volume content to withstand the mechanical over-load. Thus for each engine component, it is important to understand the probability of shock, and where it might occur in order to assure that the CMC will have sufficient overload capability in these locations to maintain component integrity and allow continuous engine operation. As discussed in Section 4.3, the use of 3D fiber architectures not only improves the mechanical shock or impact resistance of SiC/SiC panels, but also can improve the panel thru-thickness thermal conductivity, thereby reducing the stresses from any thermal shock situation.

Finally, a predictable and very important life-limiting issue for SiC/SiC components is erosion and/or corrosion of the component surface during high-temperature gas-turbine service. This effect, which can be severe for all silicon-based ceramics, is typically due to the water vapor formed in the combustion process, which reacts with the oxides, such as silica, that continually form on the ceramic surface, causing them to volatilize. This in turn results in surface recession of the ceramic at a rate that increases with water vapor pressure, combustion gas velocity, and most importantly with CMC surface temperature (Ref. 43). To minimize this effect, environmental barrier coatings (EBC) have been developed for both Si-based monolithics and composites (Refs. 44 and 45). For industrial gas turbines, these EBC have been very instrumental in extending the life of SiC/SiC CMC combustor liners and shrouds at temperatures up to ~1250 °C (Ref. 46), but little experience exists for using EBC under more aggressive engine conditions. Because EBC themselves are typically produced from oxide compositions, such as barium aluminosilicate and mullite, they generally display very low thermal conductivity, thereby also acting as thermal barrier coatings (TBC). Thus EBC are not only important for maintaining ceramic component cross-section, they can also aid in reducing the surface temperature of a cooled ceramic component by providing another source of thermal resistance between the combustion gas temperature and the component surface. Generally EBC are required for Si-based ceramic components that will require long-

time service and surface temperatures above ~1000 °C. As efforts are ongoing to increase the upper use temperatures of SiC/SiC components beyond 1250 °C, recession becomes the primary concern for long component life. Thus high-temperature EBC development is a key objective of current studies at NASA (Ref. 47).

6.0 Concluding Remarks

This chapter has detailed the results of various studies conducted primarily at the NASA Glenn Research Center aimed at advancing the current state of experimental and mechanistic knowledge concerning the constituent materials and processes for SiC/SiC composites. When compared to current approaches for SiC/SiC aero-propulsion components, this knowledge has the potential of generating components with enhanced structural reliability and higher temperature performance. It should be realized that these advancements have been demonstrated primarily using single SiC fibers, woven SiC/SiC pre-forms, and SiC/SiC test coupons removed from panels that contain the improved approaches. These specimens were then tested under simple conditions such as laboratory air, constant temperature, and constant stress along the primary fiber direction. Thus considerable more effort is required before these advancements can be comfortably implemented into real SiC/SiC engine components. Nevertheless, when compared to current approaches for SiC/SiC components, they clearly show substantial improvements, particularly for achieving the multiple engine benefits that can be accrued by components with durable higher temperature performance. Because of these benefits, efforts at NASA are on-going to further understand and demonstrate the practical viability of these advancements.

References

1. D.A. Lewis, M.T. Hogan, J. McMahon, and S. Kinney, Application of Uncooled Ceramic Matrix Composite Power Turbine Blades for Performance Improvement of Advanced Turboshaft Engines, Proceedings of the American Helicopter Society 64th Annual Forum (2008).
2. M. Mecham, Out of the Lab, *Aviation Week*, July 30, 13 (2012).
3. M.H. Jaskowiak and J.A. Setlock, Processing and Properties of Sapphire Reinforced Alumina Composites, Proceedings of the 20th Annual Conference on Ceramic, Metal, and Carbon Composites, pp. 843–862 (1997).
4. G.N. Morscher and V. Pujar, Creep and Stress-Strain Behavior after Creep for SiC Fiber- Reinforced Melt-Infiltrated SiC Matrix Composites, *J. Am. Ceram. Soc.* 89, 1652–1658 (2006).
5. J. Lang and J.A. DiCarlo, Modeling Creep-Induced Stress Relaxation at the Leading Edge of SiC/SiC Airfoils, Proceedings of the 31st Annual Conference on Ceramics, Metal &Carbon Composites, Materials and Structures, Restricted Sessions, Cape Canaveral, FL (2007).
6. J.A. DiCarlo, H.M. Yun, G.N. Morscher, and R.T Bhatt, SiC/SiC Composites for 1200 °C and Above, in *Handbook of Ceramic Composites*, N. Bansal, Ed., Kluwer Academic Publishers, Boston, pp. 77–98 (2005).
7. R.T. Bhatt and J.A. DiCarlo, Method of Improving the Thermo-Mechanical Properties of Fiber-Reinforced Silicon Carbide Matrix Composites, U.S. Patent Application.
8. G.S. Corman and K.L. Luthra, Silicon Melt-Infiltrated Ceramic Composites (HiPerComp), in *Handbook of Ceramic Composites*, N. Bansal, Ed., Kluwer Academic Publishers, Boston, pp. 99–115 (2005).
9. T. Ishikawa, Advances in Inorganic Fibers, *Adv. Polym. Sci.* 178, 109–144 (2005).
10. J.A. DiCarlo and H.M. Yun, Creep of Ceramic Fibers: Mechanisms, Models, and Composite Implications, *in Creep Deformation: Fundamentals and Applications*, R.S. Mishra, J.C. Earthman, and S.V. Raj, Eds., The Minerals, Metals, and Materials Society, Warrendale, PA, pp. 195–208 (2002).

11. M. Takeda, J. Sakamoto, A. Saeki, Y. Imai, and H. Ichikawa, High Performance Silicon Carbide Fiber Hi-Nicalon for Ceramic Matrix Composites, *Cer. Eng. Sci. Proc.*, 16 [4], 37–44 (1995).
12. H. Ichikawa, High Performance SiC Fibers from Polycarbosilane for High Temperature Applications, *Key Engineering Materials*, 352, 59–64 (2007).
13. Private communication: R.T. Bhatt.
14. H.M. Yun, D. Wheeler, Y. Chen, and J.A. DiCarlo, Thermo-Mechanical Properties of Super Sylramic SiC Fibers, *Cer. Eng. Sci. Proc.*, 26 [2], 59–65 (2005).
15. M. Takeda, J. Sakamoto, and H. Ichikawa, Mechanical and Structural Analysis of Silicon Carbide Fiber Hi-Nicalon Type S, *Cer. Eng. Sci. Proc.*, 17 [4], 35–42 (1996).
16. H.M. Yun and J.A. DiCarlo, Tensile Behavior of As-Fabricated and Burner-Rig Exposed SiC/SiC Composites With Hi-Nicalon Type S Fibers, *Cer. Eng. Sci. Proc.*, 23 [3], 571 (2002).
17. J.A. DiCarlo, SiC Fiber Creep and Rupture Models for Understanding CMC Behavior Above 1400 °C, NASA TM in preparation.
18. R.M. Cannon, W.H. Rhodes, and A.H. Heuer, Plastic Deformation of Fine-Grained Alumina: I, Interface-Controlled Diffusional Creep, *J. Am. Ceram. Soc.*, 63, [1–2] 46–53 (1979).
19. G.N. Morscher and J.A. DiCarlo, A Simple Test for Thermo-mechanical Evaluation of Ceramic Fibers. *J. Am. Ceram. Soc.*, 75, 136–40 (1992).
20. Private communication: G.N. Morscher.
21. G. Pezzotti, H.J. Kleebe, H. Nishimura, and K. Ota, Grain-Boundary Viscosity of Preoxidized and Nitrogen-Annealed Silicon Carbides, *J. Am. Ceram. Soc.*, 84 [10] 2371–76 (2001).
22. M.D. Sacks, W. Toreki, C.D. Batish, and G.J. Choi, Preparation of Boron-Doped Silicon Carbide SiC Fibers, U.S. Patent 5851942 (1998).
23. J. Lipowitz, J.A. Rabe, A. Zangvil, and Y. Xu, Structure and Properties of Sylramic™ Silicon Carbide Fiber—A Polycrystalline, Stoichiometric β–SiC Composition. *Ceram. Eng. Sci. Proc.*, 18 [3], 147–157 (1997).
24. J. Lipowitz and J.A. Rabe, Preparation of polycrystalline ceramic fibers, U.S. Patent 5279780 (1994).
25. J.A. DiCarlo and H.M. Yun, Methods for Producing Silicon Carbide Architectural Preforms, U.S. Patent 7687016 B1 (2010).
26. S.M. Dong, et al., Characterization of nearly stoichiometric SiC ceramic fibers. *J. Mat. Sci.*, 36, 2371–2381 (2001).
27. V.V. Pujar and G.N. Morscher, Tensile Creep Behavior of Melt-Infiltrated SiC Composites for Gas Turbine Engine Applications; Proceedings of ASME Turbo Expo 2007, May 14–17, Montreal, Canada, Paper GT2007-27491. Also, G.N. Morscher and V. Pujar, Design Guidelines for In-Plane Mechanical Properties of SiC Fiber-Reinforced Melt-Infiltrated SiC Composites. *Int. J. Appl. Ceram. Technol.*, 6, 151–63 (2009).
28. D. Dunn, The Effect of Fiber Volume Fraction in HiPerComp SiC-SiC Composites, PhD Thesis, Alfred, New York, 2010.
29. J.A. DiCarlo and H.M. Yun, Non-oxide (Silicon Carbide) Fibers, in *Handbook of Ceramic Composites*, N. Bansal, Ed., Kluwer Academic Publishers, Boston, pp. 33–52 (2005).
30. L. Thomas-Ogbuji, A Pervasive Mode of Oxidation Degradation in a SiC/SiC Composite, *J. Am. Ceramic Soc.*, 81, 2777-2784 (1998).
31. G.N. Morscher, H.M. Yun, J.A. DiCarlo, and L. Thomas-Ogbuji, L. (2004), Effect of a BN Interphase that Debonds Between the Interphase and the Matrix in SiC/SiC Composites, *J. Am. Ceramic Soc*., 87, 104–12 (2004). Also U.S. Patent 7427428.
32. J.A. DiCarlo and M. van Roode, Ceramic Composite Development for Gas Turbine Engine Hot Section Components. Proceedings of ASME Turbo Expo 2006: Power for Land, Sea and Air, Paper GT2006-90151, Barcelona, Spain (2006).
33. M.J. Verrilli, J.A. DiCarlo, H.M. Yun, and T.R. Barnett, Hoop Tensile Characterization of SiC/SiC Cylinders Fabricated from Spliced 2D Fabric, *Cer. Eng. Sci. Proc.*, 24 [4], 407–413 (2003).

34. H.M. Yun, J.A. DiCarlo, and R.T Bhatt, Advanced SiC/SiC Ceramic Composites for Air-Breathing and Rocket Propulsion Engine Components, Proceedings of JANNAF Conference, Charleston SC (2005).
35. H.M. Yun, J.A. DiCarlo, R.T Bhatt, and T. Easler, Advanced SiC/SiC Ceramic Composites for Hot-Section Aerospace Components, Proceedings of National Space & Missile Materials Symposium, Summerlin, NV (2005).
36. H.M. Yun, J.A. DiCarlo, R.T Bhatt, and M.H. Jaskowiak, Thermo-structural Properties of SiC/SiC Panels With 2.5D and 3D Fiber Architectures, Proceedings of the 29th Annual Conference on Ceramics, Metal &Carbon Composites, Materials and Structures, Restricted Sessions, Cape Canaveral, FL (2005).
37. G.N. Morscher, J.A. DiCarlo, J.D. Kiser, and H.M. Yun, Effects of Fiber Architecture on Matrix Cracking for Melt-Infiltrated SiC/SiC Composites. *Int. J. Appl. Ceram. Technol*., 7 [3] 276–290 (2010).
38. R.T. Bhatt, L.M. Cosgriff, and D.S. Fox, Influence of Fiber Architecture on Impact Resistance of Uncoated SiC/SiC Composites, Proceedings of 8th Pacific Rim Conference on Ceramic and Glass Technology, Vancouver, BC (2009).
39. Private communication: T.E.A.M: Textile Engineering and Manufacturing, Woonsocket, RI.
40. J.A. DiCarlo and R.T. Bhatt, Modeling SiC/SiC Creep-Rupture Behavior from 2400 to 3000 °F. Proceedings of 35th Annual Conference on Composites, Materials, and Structures, Cocoa Beach/Cape Canaveral, FL (2011).
41. G.N. Morscher, Tensile Creep of Melt-Infiltrated SiC/SiC Composites With Unbalanced Sylramic-iBN Fiber Architectures, *Int. J. Appl. Ceram. Technol*., 8 [2], 239–250 (2011).
42. R.T. Bhatt, J.A. DiCarlo, and J.D. Kiser, Tensile and Creep Properties of Hybrid CVI-PIP SiC/SiC Composites at High Temperatures in Air. Proceedings of 36th Annual Conference on Composites, Materials, and Structures, Cocoa Beach/Cape Canaveral, FL (2012).
43. J.L. Smialek, R.C. Robinson, E.J. Opila, D.S. Fox, and N.S. Jacobson, SiC and Si_3N_4 Recession Due to SiO_2 Scale Volatility under Combustor Conditions, *Adv. Composite Mater*, 8[1], pp. 33–45 (1999).
44. K.N. Lee, D.S. Fox, J.I. Eldridge, D. Zhu, R.C. Robinson, N.P. Bansal, and R.A. Miller, Upper Temperature Limit of Environmental Barrier Coatings Based on Mullite and BSAS, *J. Am. Ceram. Soc*., 86 [8] 1299–1306 (2003).
45. K.N. Lee, D.S. Fox, and N.P. Bansal, Rare Earth Silicate Environmental Barrier Coatings for SiC/SiC Composites and Si3N4 Ceramics, *J. Eur. Ceram. Soc*., 25 [10] 1705–1715 (2005).
46. M. van Roode, J.R. Price, J., Kimmel, N. Miriyala, D. Leroux, A. Fahme, and K. Smith, Ceramic Matrix Composite Combustor Liners: A Summary of Field Evaluations, *Transactions of the ASME, J. Eng. Gas Turbines & Power*, 129, 21–30 (2007).
47. Zhu, D., Miller, R.A., and Fox, D.S. (2007), Thermal and Environmental Barrier Coating Development for Advanced Propulsion Engine Systems, AIAA–2007–2130, American Institute of Aeronautics and Astronautics. Also NASA/TM—2008-215040.

REPORT DOCUMENTATION PAGE			Form Approved OMB No. 0704-0188

1. REPORT DATE *(DD-MM-YYYY)*	2. REPORT TYPE	3. DATES COVERED *(From - To)*
01-07-2013	Technical Memorandum	

4. TITLE AND SUBTITLE
Advances in SiC/SiC Composites for Aero-Propulsion

5a. CONTRACT NUMBER

5b. GRANT NUMBER

5c. PROGRAM ELEMENT NUMBER

6. AUTHOR(S)
DiCarlo, James, A.

5d. PROJECT NUMBER

5e. TASK NUMBER

5f. WORK UNIT NUMBER
WBS 694478.02.93.02.11.13.22

7. PERFORMING ORGANIZATION NAME(S) AND ADDRESS(ES)
National Aeronautics and Space Administration
John H. Glenn Research Center at Lewis Field
Cleveland, Ohio 44135-3191

8. PERFORMING ORGANIZATION REPORT NUMBER
E-18700

9. SPONSORING/MONITORING AGENCY NAME(S) AND ADDRESS(ES)
National Aeronautics and Space Administration
Washington, DC 20546-0001

10. SPONSORING/MONITOR'S ACRONYM(S)
NASA

11. SPONSORING/MONITORING REPORT NUMBER
NASA/TM-2013-217889

12. DISTRIBUTION/AVAILABILITY STATEMENT
Unclassified-Unlimited
Subject Category: 24
Available electronically at http://www.sti.nasa.gov
This publication is available from the NASA Center for AeroSpace Information, 443-757-5802

13. SUPPLEMENTARY NOTES

14. ABSTRACT
In the last decade, considerable progress has been made in the development and application of ceramic matrix composites consisting of silicon carbide (SiC) based matrices reinforced by small-diameter continuous-length SiC-based fibers. For example, these SiC/SiC composites are now in the early stages of implementation into hot-section components of civil aero-propulsion gas turbine engines, where in comparison to current metallic components they offer multiple advantages due to their lighter weight and higher temperature structural capability. For current production-ready SiC/SiC, this temperature capability for long time structural applications is ~1250 °C, which is better than ~1100 °C for the best metallic superalloys. Foreseeing that even higher structural reliability and temperature capability would continue to increase the advantages of SiC/SiC composites, progress in recent years has also been made at NASA toward improving the properties of SiC/SiC composites by optimizing the various constituent materials and geometries within composite microstructures. The primary objective of this chapter is to detail this latter progress, both fundamentally and practically, with particular emphasis on recent advancements in the materials and processes for the fiber, fiber coating, fiber architecture, and matrix, and in the design methods for incorporating these constituents into SiC/SiC microstructures with improved thermo-structural performance.

15. SUBJECT TERMS
Ceramic composites; SiC fibers; Fiber architectures; Fiber coatings; SiC matrices; SiC/SiC design

16. SECURITY CLASSIFICATION OF:			17. LIMITATION OF ABSTRACT	18. NUMBER OF PAGES	19a. NAME OF RESPONSIBLE PERSON
a. REPORT	b. ABSTRACT	c. THIS PAGE			STI Help Desk (email:help@sti.nasa.gov)
U	U	U	UU	30	19b. TELEPHONE NUMBER *(include area code)* 443-757-5802